

Geometric scaling violations in the central rapidity region of d+Au collisions at RHIC

Adrian Dumitru^a, Arata Hayashigaki^a and Jamal Jalilian-Marian^b

*^aInstitut für Theoretische Physik, J. W. Goethe Universität
Max-von-Laue Strasse 1*

D-60438 Frankfurt am Main, Germany

^bInstitute for Nuclear Theory, University of Washington, Seattle, WA 98195

Abstract

We show that geometric scaling is satisfied to good accuracy in the forward region of d+Au collisions at RHIC. Scaling violations do show up, however, at mid-rapidity, and the anomalous dimension of the small- x gluon distribution evolves to near its DGLAP limit for transverse momenta of a few GeV. This represents a first consistency check of RHIC deuteron-nucleus and HERA DIS phenomenology, and of the universality of the underlying Color Glass Condensate (CGC) theory, which describes both phenomena. It also reconciles successful leading-twist LO and NLO perturbative QCD computations of mid-rapidity particle production with small- x evolution. Finally, we introduce a new parameterization for the anomalous dimension of the small- x gluon distribution which properly reproduces known theoretical limits at large rapidity, at large virtuality, and on the saturation boundary, and still fits the available data from d+Au collisions at RHIC. We find indications that sub-asymptotic terms in the rapidity-evolution of the anomalous dimension are large.

1 Introduction

The weak-coupling gluon saturation formalism [1, 2] has been used at HERA, rather successfully, in order to describe the x and Q^2 dependence of the inclusive proton structure function $F_2(x, Q^2)$. Specifically, the simple Golec-Biernat and Wüsthoff (GBW) model [3] provided a very efficient qualitative “summary” of the small- x , moderate Q^2 data in terms of an initial condition $Q_s^2(x_0) = Q_0^2$ for the saturation momentum and its (constant) growth rate $\lambda = \partial \log Q_s^2 / \partial \log 1/x$. It led to the discovery of the interesting phenomenon of “geometric scaling” [4], implying that in the relevant range of x and Q^2 , the structure function depends on x and Q^2 exclusively via the scaling variable $Q^2/Q_s^2(x)$. In other words, that the scattering cross section for a dipole of size r_t does not depend on r_t and x separately but only through the combination $\rho = r_t Q_s(x)$.

This phenomenon does not find a natural explanation within the linear Dokshitzer, Gribov, Lipatov, Altarelli, Parisi (DGLAP) [5] and Balitsky, Fadin, Kuraev, Lipatov (BFKL) [6] QCD evolution equations in the absence of saturation boundary conditions. It has been shown to arise from the BFKL equation *with* saturation boundary conditions [7], in an expansion of the LO-BFKL solution to first order about the saturation line, and in mean-field approximation. That equation, with the corresponding boundary condition, represents an approximation to the full non-linear “Color Glass Condensate” (CGC) theory of QCD evolution. It is valid only on one side of the saturation line $Q_s(x)$, in the dilute regime.

Moreover, refs. [7] also computed the *scaling violations*¹ which emerge away from the saturation boundary at $Q^2 \gg Q_s^2(x)$. They arise from the diffusion term in the expansion of the LO-BFKL solution to second order about the saturation saddle-point, which shifts the anomalous dimension γ of the target gluon distribution by $\Delta\gamma \sim y^{-1} \log(1/r_t Q_s(y))$ as one moves away from the saturation boundary ($y = \log 1/x$ denotes rapidity). By $Q_{gs}^2(x) \sim Q_s^4(x)/\Lambda^2$, scaling violations grow to order one (Λ is a non-perturbative scale in the infrared, of order Λ_{QCD}); Q_{gs} is the upper boundary of the so-called geometric scaling window. Beyond this virtuality, the target gluon distribution is described for example by the DLA form, if y and $\log Q^2$ are sufficiently large.

A fit to the HERA data in the “extended” geometric scaling window $Q_s^2(x) < Q^2 < Q_{gs}^2(x)$ has been performed by Iancu, Itakura and Munier (IIM) in ref. [8] (see also [9]), employing a dipole model which represents an approximate solution to the JIMWLK equations [10] governing the mean-field evolution of color dipoles. They find evidence for scaling violations in the HERA data, as predicted by the CGC theory: a substantial increase of γ with $1/r_t$ is required to improve the agreement with the data as compared to the original GBW dipole model.

In recent years, new data on single-inclusive hadron production at semi-hard transverse momenta emerged from the Relativistic Heavy-Ion Collider (RHIC). Here, we are interested in particular in data from deuteron-gold collisions at central and forward rapidity (toward the fragmentation region of the deuteron projectile) [11, 12, 13, 14], which may probe

¹We shall use this terminology throughout the manuscript to refer to violations of *geometric scaling* away from the saturation line, not to the violation of Q^2 scaling due to DGLAP evolution.

high gluon densities in the gold target, and at the same time, should be less affected by final-state effects than nucleus-nucleus collisions.

A first semi-quantitative analysis of the d+Au data from RHIC was performed by Kharzeev, Kovchegov and Tuchin (KKT) in ref. [15], identifying qualitative features of the expected CGC evolution and providing an alternative dipole parameterization: the KKT model, to be described below, was constructed to fit RHIC instead of HERA data. In ref. [16], we extended the standard CGC approach to particle production to include recoil effects of the large- x projectile partons, and found very good quantitative agreement with RHIC data at large rapidity using either the KKT or the IIM dipole. It turned out that a crucial feature of both dipole models lies in the fact that the target anomalous dimension at large rapidity and moderate p_t is essentially constant, $\gamma \approx 0.6$, and substantially smaller than in the DGLAP regime ($\gamma_{DGLAP} \sim 1$). Hence, for transverse momenta of a few GeV and rapidity $y_h \gtrsim 3$, the data points are in either the saturation or extended scaling regions, where scaling violations are essentially *absent* at RHIC energy.

In the present paper, we extend our previous calculation of forward hadron production [16] to the mid rapidity region. Our main objective is to analyze whether scaling violations, as predicted by the CGC theory and previous dipole fits to HERA data, show up. This is a necessary condition for establishing the CGC as a universal theory of QCD evolution near a saturation boundary within the weak-coupling (semi-hard) regime.

The paper is organized as follows. In the next section, we introduce the formula for the single-inclusive hadron production cross section in high-energy proton (or deuteron) collisions with a heavy nucleus which accounts for both small- x evolution of the dense target and full DGLAP evolution of the dilute projectile. We also present the KKT dipole parameterization there. In section 3 we apply this formalism to hadron production at mid-rapidity and compare to data from RHIC to check for the presence of scaling violations. In section 4 we modify the IIM dipole parameterization, in particular that of the anomalous dimension, to fit the available data from RHIC at central and at forward rapidity, which is done in section 5. Finally, section 6 contains our summary and conclusion.

2 Proton-Nucleus Collisions within the CGC approach

The single-inclusive hadron production cross section in p+A collision is given by [16]

$$x_F \frac{d\sigma^{pA \rightarrow hX}}{dx_F d^2p_t d^2b} = \frac{1}{(2\pi)^2} \int_{x_F}^1 dx_p \frac{x_p}{x_F} \left[f_{q/p}(x_p, Q_f^2) N_F \left(\frac{x_p}{x_F} p_t, b \right) D_{h/q} \left(\frac{x_F}{x_p}, Q_f^2 \right) + f_{g/p}(x_p, Q_f^2) N_A \left(\frac{x_p}{x_F} p_t, b \right) D_{h/g} \left(\frac{x_F}{x_p}, Q_f^2 \right) \right], \quad (1)$$

where p_t and x_F are the transverse momentum and the Feynman- x of the produced hadron, respectively. x_p denotes the momentum fraction of a projectile parton and b is the impact parameter. Note that this expression is different from the more common K_\perp factorized

expressions [6, 17] in that *the radiation vertex is exact*. The common eikonal (soft gluon) approximation made in the K_\perp factorization approach is omitted, which reflects in the fact that the projectile parton distribution functions $f(x_p, Q_f^2)$, and their fragmentation functions $D(z, Q_f^2)$ into hadrons, evolve according to the full DGLAP [5] evolution equations and respect the momentum sum-rule. The importance of this evolution for the interpretation of forward-rapidity data from RHIC is discussed in detail in [16]. One should keep in mind, however, that eq. (1) is valid only in the limit of high parton energy and for a dilute projectile. It resums large logarithms arising from evolution of the target wave function with x as well as from evolution of the collinearly factorized projectile quark and gluon distributions with Q^2 .

The cross section depends on the scattering probability of dipoles of size r_t in the fundamental and adjoint representations, respectively, at an impact parameter b :

$$\begin{aligned} N_F(r_t, b) &\equiv \frac{1}{N_c} \text{Tr}_c \langle 1 - V^\dagger(b - r_t/2)V(b + r_t/2) \rangle, \\ N_A(r_t, b) &\equiv \frac{1}{N_c^2 - 1} \text{Tr}_c \langle 1 - U^\dagger(b - r_t/2)U(b + r_t/2) \rangle, \end{aligned} \quad (2)$$

where V and U denote Wilson lines along the light cone [10] in the corresponding representation, and N_c is the number of colors.

In practice, the ab-initio determination of dipole profiles by solution of the JIMWLK equations is not feasible yet. Therefore, one resorts to theory-motivated phenomenological parametrizations of the dipole profile which can be tested against data. An example is the KKT model [15], where the dipole profile is parameterized as

$$N_A(r_t, y_h) = 1 - \exp \left[-\frac{1}{4} (r_t^2 Q_s^2(y_h))^{\gamma(y_h, r_t)} \right], \quad (3)$$

with y_h the rapidity of the produced hadron. The saturation scale of the nucleus at y_h is given as²

$$Q_s(y_h) = Q_0 \exp[\lambda(y_h - y_0)/2]. \quad (4)$$

Here, $\lambda \simeq 0.3$ is fixed by the DIS data and the initial condition $Q_0 \simeq 1$ GeV is set at $y_0 = 0.6$, where small- x quantum evolution becomes effective. The saturation scale for the dipole in the fundamental representation differs by a factor of $Q_s^2 \rightarrow Q_s^2 C_F/C_A = \frac{4}{9} Q_s^2$.

γ denotes the anomalous dimension of the target gluon distribution with saturation boundary condition and is modeled by KKT as

$$\gamma(y_h, q_t) = \frac{1}{2} \left(1 + \frac{|\xi(y_h, q_t)|}{|\xi(y_h, q_t)| + \sqrt{2|\xi(y_h, q_t)|} + 7 c \zeta(3)} \right). \quad (5)$$

²Note that if hadron masses and intrinsic transverse momenta from fragmentation are neglected, then the rapidity of the produced hadron equals that of its parent parton. Hence, we do not distinguish between them.

Here, we have written γ as a function of transverse momentum rather than dipole size by evaluating it at a characteristic value $r_t \sim 1/q_t$. The free parameter c in (5) governs the onset of the quantum evolution regime, and has been fixed by KKT to $c = 4$.

The *Ansatz* (3) exhibits geometric scaling when γ is constant. Scaling violations are introduced into the KKT parameterization through the function

$$\xi(y_h, q_t) = \frac{\log(q_t^2/Q_0^2)}{(\lambda/2)(y_h - y_0)}. \quad (6)$$

ξ vanishes as $y_h \rightarrow \infty$ at fixed q_t , so that $\gamma \rightarrow 1/2$. On the other hand, approaching the saturation boundary at large rapidity far from the initial condition (i.e. $q_t \rightarrow Q_s(y_h)$ for $y_h \gg y_0$) leads to $\xi \rightarrow 2$. Due to the last term in the denominator of eq. (5) this corresponds to $\gamma \approx 0.53$, again close to the usual BFKL saddle point *without* saturation boundary conditions.

3 Scaling violations in the mid-rapidity RHIC data

It was shown in ref. [16] that the BRAHMS data [11] on forward hadron production from d+Au collisions at RHIC are described very well³ by both the KKT [15] and the IIM [8] dipoles, provided that DGLAP evolution of the dilute projectile with exact splitting functions is taken into account. The predictions made in [16] appear to be confirmed by the preliminary data from STAR on π^0 production at rapidity $y_h \simeq 4$ [12]. The fact that both dipole parameterizations generically include an anomalous dimension of the target gluon distribution that *differs* from 1 at small x_A proved crucial. In particular, for $y_h \gtrsim 3$ both KKT and IIM dipoles predict a nearly p_t -independent anomalous dimension $\gamma \approx 0.6$ for $p_t \lesssim 10$ GeV, which is close to the LO-BFKL prediction⁴ of $\gamma = \gamma_s \approx 0.627$ and, with eq. (1) from above, is consistent with the experimental p_t distributions [16].

In the present paper, we consider particle production in the central region, $y_h = 0$. As we shall see, here the behavior of γ required by the data and the CGC approach is very different. Before comparing to data, however, it is useful to analyze the kinematics. While forward hadron production probes rather small x_A in the target nucleus [16], one may wonder to what extent the conditions for applicability of the CGC formalism are met in mid-rapidity, for RHIC energy ($\sqrt{s} = 200$ GeV). We expect that the CGC description breaks down beyond some x_0 , where recoil effects affect the evolution with $\log 1/x$. Near x_0 , knowledge of the *width* $\Delta x/x_0$ of that transition region would also be required. Neither x_0 nor Δx can be determined from the CGC formalism itself, since we presently lack a treatment of recoil and of other “large- x ” effects within this approach.

However, since evolution in x appears to be quite rapid, it is probably not a bad approximation to consider just one value of x beyond which the CGC small- x formalism will

³Already at leading order in α_s , if a phenomenological p_t -independent K -factor for NLO corrections is allowed for.

⁴This is the anomalous dimension for BFKL evolution with saturation boundary condition, i.e. for evolution along the saturation line.

break down. Experimentally, it is known that HERA data on proton structure functions at or below $x_0 \sim 0.01$ can be described reasonably well within the small- x evolution approximation [3, 4, 8, 9]. In case of nuclear targets, larger values of x_0 are expected due to the $\sim A^{1/3}$ enhancement of the saturation scale near x_0 [18]. Therefore, for a rough estimate, we take $x_0 = 0.05$ as the upper limit of validity of the small- x approximation. Below, we shall check the kinematic region contributing to the cross section for mid-rapidity hadron production at RHIC.

At $y_h = 0$, the projectile and target x are equal and given by $x = q_t/\sqrt{s}$, with q_t the transverse momentum of the produced parton. If we assume that the small- x approximation of the CGC can be applied for $x < x_0 \simeq 0.05$, then this translates into transverse momenta up to $q_t \simeq 0.05\sqrt{s}$. Hence, for RHIC energy the approach should be valid for $q_t \lesssim 10$ GeV, extending to $q_t \lesssim 300$ GeV for $\sqrt{s} = 6$ TeV p+A collisions at the LHC. Hadronization reduces this number by a factor of ≈ 0.7 (≈ 0.5) at RHIC (LHC) energy, according to the typical values of $z = x_F/x_p$ in the fragmentation. Hence, we estimate that the formalism can be applied to hadron production in the central region at RHIC energy for hadron transverse momenta up to $p_t \simeq 7$ GeV.

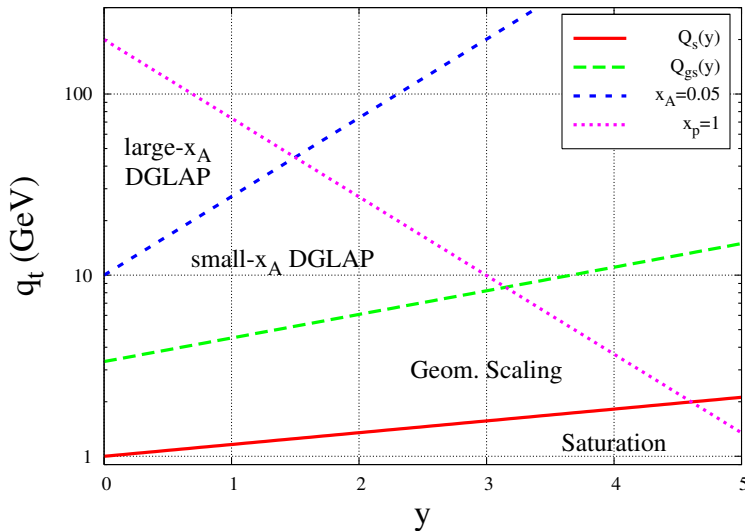


Figure 1: Schematic “phase diagram” of pA collisions at RHIC. For this plot, we have simply assumed that $Q_s(y) = 1 \text{ GeV} \times \exp(\lambda y/2)$ and $Q_{gs}(y) = Q_s^2(y)/300 \text{ MeV}$; see, however, sections 4 and 5.

This upper limit for the small- x approximation is above the boundary between the extended scaling and the dilute DGLAP regimes, $Q_{gs} \sim Q_s^2(y)/\Lambda$ [7]. With $Q_s^2 \simeq 1 \text{ GeV}^2$ at mid-rapidity (averaged over the transverse plane and at RHIC energy) and $\Lambda = 200 \text{ MeV}$, this boundary occurs at a parton transverse momentum of about $q_t \simeq 5 \text{ GeV}$ (or hadron transverse momentum $p_t \simeq 3.5 \text{ GeV}$); with $\Lambda = 300 \text{ MeV}$, this is $q_t \simeq 3.3 \text{ GeV}$ or $p_t \simeq 2.2 \text{ GeV}$. By this q_t , the anomalous dimension of the target gluon distribution should already have approached its DGLAP limit, starting from $\gamma = \gamma_s$ at $q_t = Q_s \simeq 1 \text{ GeV}$.

Hence, we expect large scaling violations in the central region of p+A collisions at RHIC already for transverse momenta on the order of a few GeV, signaling the approach towards the DGLAP regime. At somewhat higher $q_t \gtrsim 10$ GeV finally, the small- x approximation to QCD evolution should break down, as discussed above; the high- p_t regime must be treated within full DGLAP with exact splitting functions. These different kinematical regimes are summarized in Figure 1.

These estimates are in qualitative agreement with the results of Accardi and Gyulassy [19]. They find that a resummation of the Glauber multiple-scattering series (which basically corresponds to semi-classical saturation) is required at $p_t \sim 1$ GeV, and that a rapid transition to the DGLAP regime occurs towards higher transverse momenta. Comparing their approach to data from RHIC, they do not seem to find evidence for a broad geometric scaling window. In this vein, we also recall that a purely semi-classical model without quantum evolution does not reproduce the RHIC mid-rapidity data, as shown in [20]⁵.

Similarly, leading-twist NLO pQCD [21] provides an accurate description of the mid-rapidity cross-section for $p_t \gtrsim 5$ GeV. We point out that while this indeed contradicts the original GBW model, it is perfectly consistent with improved HERA fits including scaling violations [8] and with the CGC theory, which does predict that $\gamma \rightarrow \sim 1$ for $q_t > Q_{gs}$. That this is perhaps the correct interpretation can be inferred from the *suppression* of scaling violations at large rapidity (and $p_t \sim$ few GeV), which again is a generic prediction of the CGC approach⁶, and has already been verified to be consistent with RHIC data [16].

For p+A collisions at the LHC, at midrapidity the extended scaling window terminates roughly at $q_t \simeq 20$ GeV (using an average $Q_s^2 \simeq 4$ GeV²), which is about an order of magnitude less than our estimate for the transverse momentum where “large- x ” effects such as recoil become important. Hence, here a much wider window $10 \lesssim p_t \lesssim 150$ GeV for the small- x approximation in the dilute regime exists. In the geometric scaling window below $p_t \sim 10$ GeV we expect suppression of particle production relative to the leading-twist, collinearly factorized pQCD limit, as suggested in Ref. [23] (originally thought to occur already at RHIC energy).

These considerations are, of course, rather qualitative and carry some uncertainties. Nevertheless, the essential conclusion for us is that it is not unreasonable to assume that a window of semi-hard transverse momenta exists in mid rapidity where the small- x approximation to evolution applies, and where the CGC formalism predicts large scaling violations. This shall be checked against RHIC data below.

To verify the requirement $x < x_0 \simeq 0.05$ in the central region at RHIC energy, we show the range of x contributing to single hadron production as obtained from eq. (1) in Fig. 2. We observe that, indeed, the typical x contributing to the cross section is not too large, ≈ 0.023 at hadron transverse momentum of $p_t = 3$ GeV. This provides some confidence that we may proceed to analyze mid-rapidity data from deuteron-gold collisions at RHIC energy in the regime of semi-hard transverse momenta.

⁵A fit is possible if one assumes an ad-hoc large “non-perturbative” contribution to Q_s , which has to be dropped again in the forward region. A critical discussion of this issue is given in ref. [20].

⁶Deriving from the fact that $\Delta\gamma \sim 1/y$ at fixed p_t . See also refs. [22].

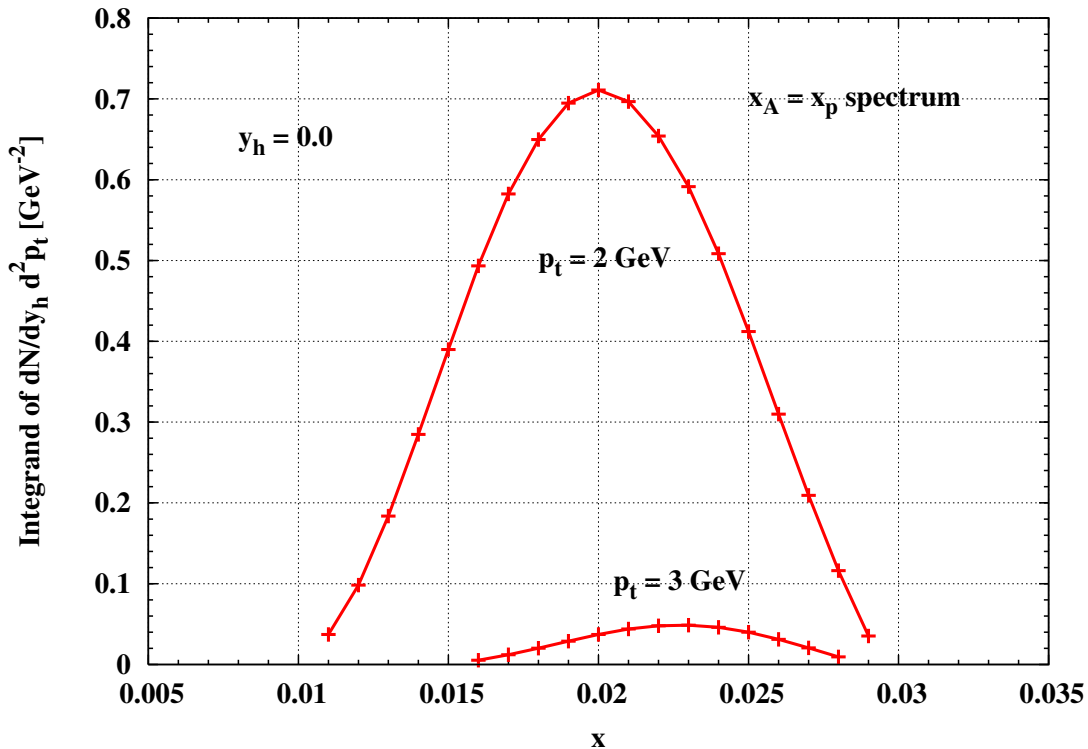


Figure 2: The range of x contributing to the cross section at mid-rapidity (RHIC energy) for hadron transverse momentum $p_t = 2$ and 3 GeV.

In Fig. 3 we show the transverse momentum spectra of charged hadrons at mid-rapidity for minimum-bias d+Au collisions at RHIC⁷. We also show the theory curves obtained from eq. (1), using CTEQ5-LO [24] parton distribution functions for the projectile deuteron, and KKP-LO [25] fragmentation functions at the scale $Q_f = p_t$. We plot curves for various *fixed* anomalous dimensions from $\gamma = 0.5$ to 0.9. Clearly, a rather steep rise of the anomalous dimension in the $p_t \sim 1 - 4$ GeV range is required for a satisfactory description of the mid-rapidity data. At the lower end, $p_t \approx 1$ GeV, the anomalous dimension is close to 0.6, perhaps marking the onset of saturation dynamics in the weak-coupling regime. This observation is further supported by the fact that saturation based models successfully describe the hadron multiplicities at RHIC, which are dominated by soft hadrons [17]. On the other hand, at $p_t = 4$ GeV, the anomalous dimension $\gamma \approx 0.9$ required to fit the data nearly equals its leading twist DGLAP limit of 1.

To illustrate this further, we plot the transverse momentum dependence of γ for the KKT model in Fig. 4. For large transverse momenta, we assume that the Fourier transform of $N_A(r_t)$ is dominated by transverse distances of order $1/q_t \sim 1/(2p_t)$ and hence evaluate $\gamma(r_t)$ at $r_t = 1/(2p_t)$.

One observes that the KKT parameterization of the anomalous dimension does not vary

⁷For better visibility, we show only the BRAHMS [11] and STAR [13] results. Data at central rapidity has also been obtained by the PHENIX [14] collaboration.

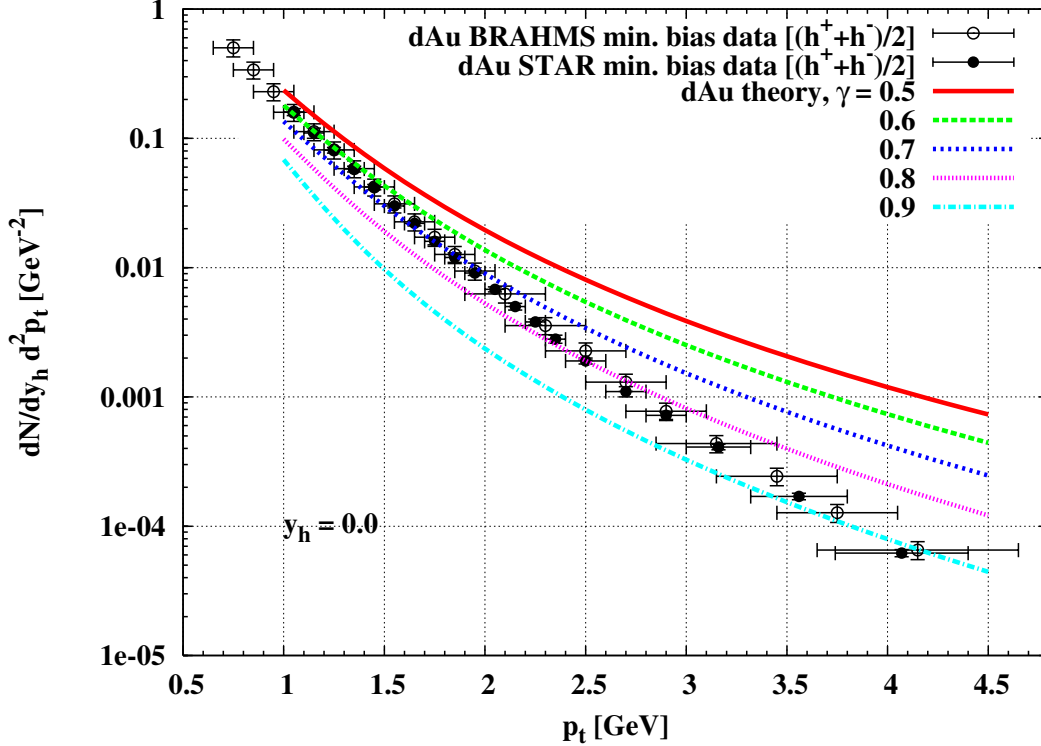


Figure 3: Charged hadron p_t spectrum obtained from eq. (1) using the KKT dipole for various fixed anomalous dimensions γ . The points with error bars show the BRAHMS [11] and STAR [13] data for minimum-bias d+Au collisions (RHIC, mid-rapidity).

much with transverse momentum, staying within $\approx 20\%$ of $\gamma \approx 0.6$. As discussed above, this behavior is generic to the CGC at *large rapidity* (i.e. small x_A), and is consistent with the RHIC data [16]. However, we have also seen that the data requires a rapid approach towards the DGLAP regime at mid-rapidity and $p_t \sim 4$ GeV, while $\gamma_{KKT} \rightarrow 1$ only at asymptotically high p_t . In other words, we find evidence for substantial scaling violations at mid-rapidity, larger than those incorporated into the KKT parameterization but in agreement with our estimates on Q_{gs} from above, which then weaken at large rapidity (they get pushed to higher p_t). Hence, the qualitative behavior of γ implied by the RHIC data is remarkably consistent both with HERA phenomenology and with the predictions of the CGC approach.

4 New parameterization of the anomalous dimension

Motivated by these results, we introduce a new parameterization of the dipole profile with an anomalous dimension incorporating stronger scaling violations than the KKT dipole. At the same time, it corrects some deficiencies of the IIM dipole at large Q^2 . In our

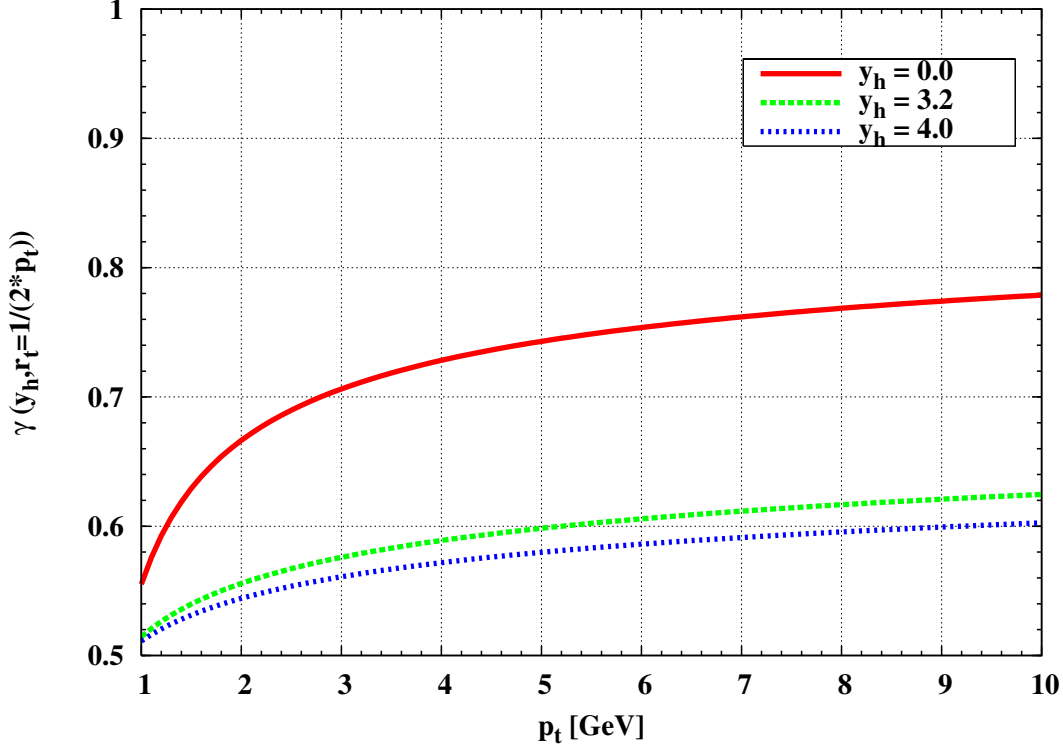


Figure 4: Anomalous dimension $\gamma(y_h, r_t)$ of the small- x nuclear gluon distribution for the KKT dipole model, evaluated at $r_t = 1/(2p_t)$.

parameterization, the anomalous dimension is given by

$$\begin{aligned} \gamma(Q^2, Y) &= \gamma_s + \Delta\gamma(Q^2, Y) \\ \Delta\gamma &= (1 - \gamma_s) \frac{\log(Q^2/Q_s^2)}{\lambda Y + \log(Q^2/Q_s^2) + d\sqrt{Y}}. \end{aligned} \quad (7)$$

We have written γ in terms of the variables appropriate for DIS, i.e. Q^2 and $Y = \log(1/x)$, similar to the GBW and IIM models. Here, $Q^2 \equiv 1/r_t^2$ is the *inverse transverse size of the dipole*, not to be confused with the factorization scale which enters the parton distribution and fragmentation functions in eq. (1). We shall transform into the variables appropriate for hadron-hadron collisions shortly.

The function is constructed such as to satisfy the following limits:

1. at any fixed rapidity Y , $\gamma \rightarrow 1$ for $Q^2 \rightarrow \infty$.
2. if $Y \rightarrow \infty$ at fixed $Q^2/Q_s^2(Y)$, $\Delta\gamma$ decreases asymptotically like $\sim 1/Y$, as determined by BFKL [8]. This indicates that the geometric scaling window broadens with Y .
3. $\gamma \rightarrow \gamma_s$ for $Q^2 \rightarrow Q_s^2(Y)$ at any rapidity.

4. At large but fixed rapidity, $Y \gg (d/\lambda)^2$, the geometric scaling window reaches up to $\log Q_{gs}^2/Q_s^2(Y) \sim \lambda Y$, consistent with the asymptotic estimate for the geometric scaling window [7]: $Q_{gs}^2 \sim Q_s^4(Y)/\Lambda_{QCD}^2$.

This last condition is the most essential difference between our new parameterization and the IIM parameterization [8], where

$$\gamma_{IIM}(Q^2, Y) = \gamma_s + \frac{\log(Q^2/Q_s^2)}{\kappa \lambda Y}. \quad (8)$$

Here, one finds $\log Q_{gs}^2/Q_s^2(Y) \sim (1 - \gamma_s)\kappa\lambda Y$, with $\kappa \simeq 10$. Hence, at large Y , their Q_{gs}^2 is much larger than $Q_s^4(Y)/\Lambda^2$. Such behavior arises if the geometric scaling window is estimated from the diffusion term in the expansion of the LO-BFKL solution to second order about the saturation saddle-point. On the other hand, if Q_{gs}^2 is estimated via the transition point between the LLA and DLA saddle points, respectively, one finds $\log Q_{gs}^2/Q_s^2(Y) \sim \lambda Y$, without the additional factor of κ (for more details see, for example, section 2.4.3 in ref. [2] and references therein).

With $\kappa\lambda Y$ replaced by λY , however, $\Delta\gamma$ rises too rapidly with $\log Q^2$ to allow for a good description of the mid-rapidity RHIC data. Also, one should keep in mind that the IIM parameterization in fact provides a good fit to the HERA data on $F_2(x, Q^2)$ at small x . Hence, strong modifications of γ are not desirable. As a consequence, to restore (approximate) agreement with the IIM parameterization, we are led to introduce terms which are subleading in Y . This agrees with indications from studies of small- x evolution equations which show that at realistic energies (rapidities), subleading corrections to the asymptotic expressions are quite large. In (7), these are modeled by the \sqrt{Y} term with a free coefficient. From the mid-rapidity RHIC data, we extract $d \simeq 1.2$ (see next section).

Fig. 5 compares our dipole parameterization (7) with $d = 1.2$ to that from eq. (8). At small x they are very similar as γ becomes flatter and approaches γ_s . Towards large x , γ is somewhat smaller for our parameterization⁸. At the same time, the new anomalous dimension is closer to 1 than γ_{KKT} , shown in Fig. 4⁹, i.e. our parameterization features a narrower scaling window. With $d = 1.2$, which restores agreement with the IIM dipole at $x = 10^{-3}$ and also describes the RHIC d+Au data correctly, the subleading term in the rapidity evolution of γ actually dominates until $Y \simeq (d/\lambda)^2 = 16$.

Finally, we also point to another recent parameterization of the dipole profile in ref. [20], which is meant to reproduce the RHIC data. That parameterization also includes breaking of geometric scaling at mid-rapidity, but not the sub-asymptotic terms for the evolution with rapidity. The dipole profile at large rapidity again resembles the KKT, IIM, and our present dipole model and so the forward hadron spectra “generated” by all these parameterizations should be rather similar.

⁸Ref. [8] considered only the region $x < 0.01$ and the fact that γ_{IIM} is not bounded from above was irrelevant for their analysis.

⁹Note also the factor of 2 difference in the p_t -scale at which γ is evaluated.

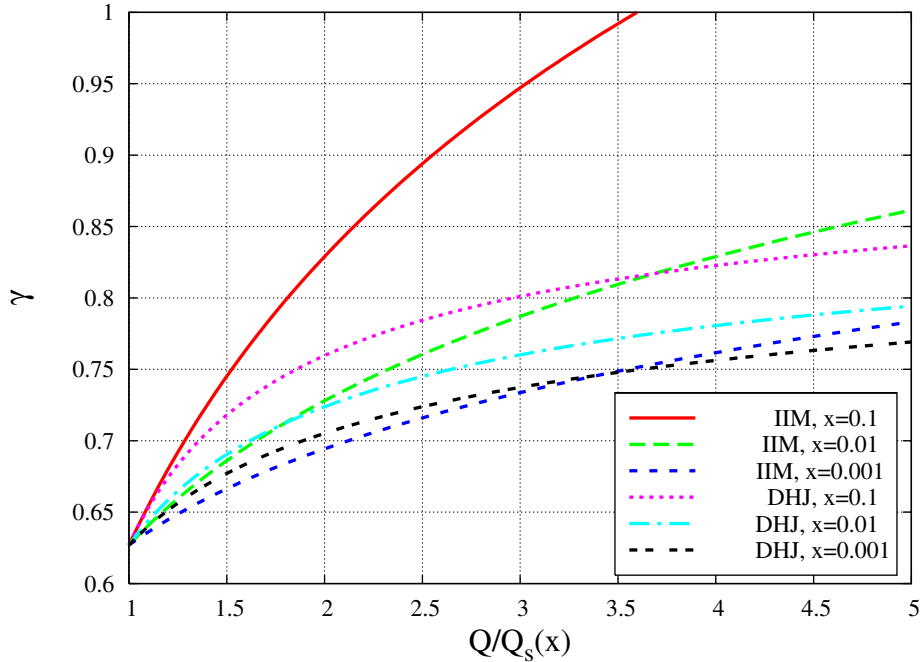


Figure 5: Anomalous dimension versus Q at various x .

5 Application to d+Au collisions at RHIC

For hadron-hadron collisions, we need to replace $Q^2 \rightarrow 1/r_t^2$ and Fourier transform the dipole profile function from (3):

$$N_{A,F}(q_t) = \int d^2r_t e^{i\vec{q}_t \cdot \vec{r}_t} N_{A,F}(r_t) = 2\pi \int_0^\infty dr_t r_t J_0(r_t q_t) N_{A,F}(r_t). \quad (9)$$

Unfortunately, it is very challenging to perform this Fourier transform numerically when γ is not constant but r_t -dependent. It is therefore common to replace $\gamma(r_t)$ by a constant $\gamma(r_t = 1/q_t)$, which makes the Fourier transform tractable [15, 16]. This is a reasonable approximation in the region where $\gamma(r_t)$ is rather flat, e.g. at large rapidity and $p_t \ll Q_{gs}$. On the other hand, at mid-rapidity, where scaling violations are larger, we found that it is important to account for the r_t -dependence of the anomalous dimension, as this strongly affects $N(q_t)$.

However, with a r_t -dependent anomalous dimension, we were unable to perform the Fourier transform (9) numerically at very large transverse momentum, where the phase factor oscillates extremely rapidly. More importantly, the Fourier transform turns negative already at intermediate q_t (≈ 8 GeV for gluons in mid rapidity), where our numerical methods are still reliable. This unphysical behavior occurs for all of the above-mentioned $\gamma(r_t)$ parameterizations (KKT, IIM and ours) and presumably indicates that the behavior of the function at very small r_t is inadequate¹⁰. We are nevertheless able to determine the

¹⁰This problem was encountered also in earlier studies [26] of Fourier transforms of the Bartels *et al.*

transverse momentum spectrum of hadrons reliably up to about $p_t = 4$ GeV, which doesn't receive contributions from the unphysical oscillations of $N_A(q_t)$ at high parton momentum. As discussed in sec. 3, we do not expect that the small- x evolution approach is valid much beyond this p_t at RHIC (mid rapidity) anyways.

The field of the target nucleus is probed at the rapidity y_A given by $y_A = \log(1/x_A) = \log(1/x_p) + 2y_h$ (see appendix B in [16] for details of kinematic definitions). Hence, the saturation scale is defined at that rapidity,

$$Q_s^2(x_A) = Q_0^2 A_{\text{eff}}^{1/3} (x_0/x_A)^\lambda . \quad (10)$$

This implies that at fixed hadron rapidity y_h , as we sum the contributions from projectile partons with different momentum fractions x_p in eq. (1), $Q_s(x_A)$ also varies.

The effective mass number of the nucleus depends on the impact parameter; following ref. [15], for heavy $A \sim 200$ targets we do not perform the integral over b explicitly but take $A_{\text{eff}} = 18.5$ for minimum bias collisions (the issue of impact parameter averaging is also discussed in ref. [20]). We fix the scale $x_0 = 3 \cdot 10^{-4}$ to the value extracted in [3] by a fit to HERA data. With $Q_0 = 1$ GeV, one obtains $Q_s \simeq 1$ GeV at mid-rapidity for transverse momenta ~ 1 GeV, which is reasonable [15].

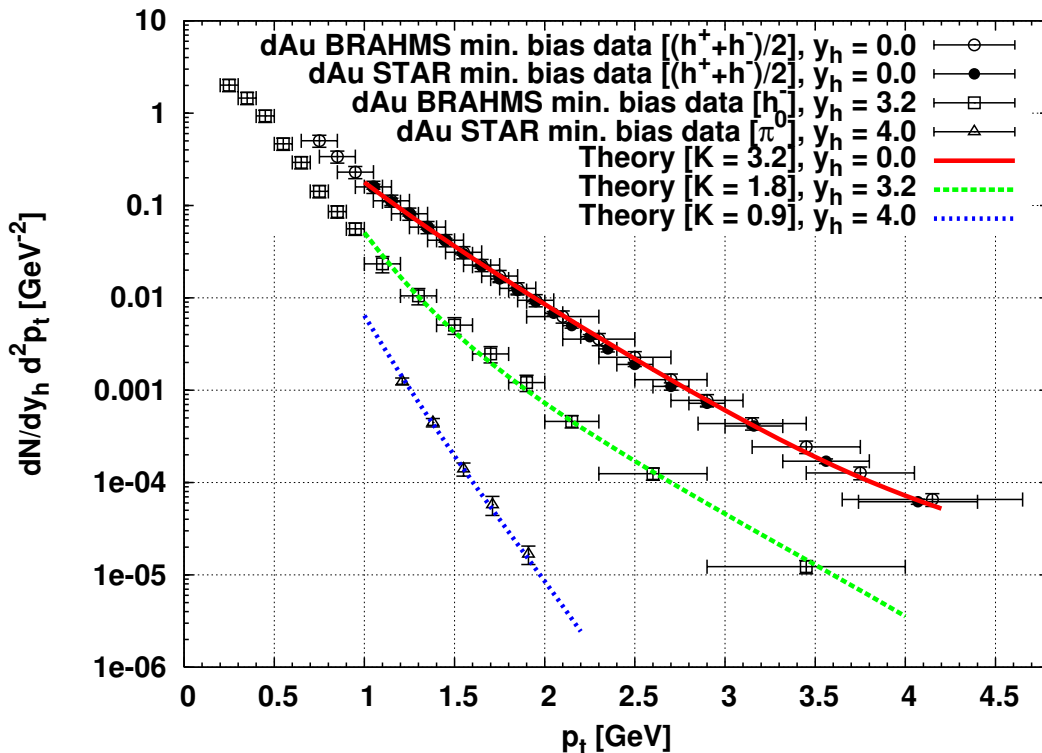


Figure 6: Comparison of theory and data for minimum-bias d+Au collisions at RHIC energy.

DGLAP-improved dipole profile [3].

In Fig. 6 we show our results for minimum-bias d+Au collisions at RHIC energy with the new parameterization (7). The factorization scale in eq. (1) is taken as $Q_f = p_t$ for all rapidities. All other parameters have been fixed above. As promised, the shape of the mid-rapidity p_t -distribution is described quite well. For the correct overall normalization, we need to multiply our LO calculation by a factor $K_{y=0} \simeq 3$. This is much larger than at forward rapidity, where $K_{y=3} \simeq 2$ and $K_{y=4} \simeq 1$, respectively (for the same scale $Q_f = p_t$ and the same parton distribution [24] and fragmentation [25] functions). Such a rapid increase of the K -factor towards mid-rapidity is expected because of larger phase space for NLO corrections¹¹. Despite the good agreement of the LO curve with the p_t -dependence of the data, NLO calculations of particle production are clearly desirable.

Fig. 6 also shows that the new parameterization of the anomalous dimension introduced here describes the forward data as well as the IIM and KKT dipole models (for the latter, see curves in [16]). As already alluded to above, the reason for this generic behavior is that all models predict a rather flat $\gamma(r_t) \approx \gamma_s$ at small x (wide geometric scaling window), and hence do not differ much. This also reflects in the fact that the forward rapidity curves from Fig. 6, which were obtained with the r_t -dependent anomalous dimension, are quite similar to those shown in ref. [16], which employed a constant $\gamma = \gamma(r_t = 1/2p_t)$. We stress that such good agreement with the data in the forward region is only achieved if the projectile parton distributions satisfy DGLAP evolution with *exact* rather than small- x approximated splitting functions [16].

6 Summary

In summary, in this paper we extended our previous studies of forward rapidity hadron production in deuteron-gold collisions at RHIC to the central rapidity region. We argued that here the CGC predicts significantly larger scaling violations than at forward rapidity, and that indeed a relatively rapid transition of the anomalous dimension of the target gluon distribution from $\gamma_s \approx 0.63$ (BFKL with saturation boundary conditions) to $\gamma \rightarrow 1$ (DGLAP) is required by the data. It is important to note that this transition occurs in a regime where the small- x approximation made in the Color Glass Condensate formalism is still valid. Hence, the scaling violations predicted by the CGC can indeed be tested.

We propose a new parameterization of the dipole profile which features a steeper transverse momentum dependence than the KKT dipole and leads to a satisfactory description of the mid-rapidity data. This agreement supports the predictions of the Color Glass Condensate formalism regarding the existence of different kinematic regions with different underlying physics.

Schematically, at small transverse momentum one probes the saturation region of the nucleus, where the underlying physics is that of a “black” target. As the transverse momentum increases, there is a transition from the saturation to the (extended) geometric scaling regime, corresponding to an anomalous dimension close to that from BFKL with saturation boundary condition. A further increase in the transverse momentum takes one

¹¹This trend is also present in pQCD calculations of hadron spectra in proton-proton collisions [27].

beyond the geometric scaling region, signaled by the necessity of introducing rather large scaling breaking in the dipole profile. We showed that for transverse momenta of about 4 GeV, one is already in a small- x DGLAP regime. Thus, the transition from the saturation to the DGLAP regions is quite narrow in the central rapidity region at RHIC. On the other hand, in the forward rapidity region ($y_h \gtrsim 3$), only the saturation and scaling regions remain, while the DGLAP window is cut off by finite-energy constraints. At LHC energy, all these kinematic regimes extend to even higher p_t , providing a great opportunity to study the various “phases” of high-energy QCD in more detail and with better accuracy.

Acknowledgements

We would like to thank W. Vogelsang for helpful discussions. J.J-M. is supported in part by the U.S. Department of Energy under Grant No. DE-FG02-00ER41132.

References

- [1] for recent reviews see, for example, A. H. Mueller, Nucl. Phys. A **715**, 20 (2003); E. Iancu and R. Venugopalan, hep-ph/0303204; L. McLerran, Nucl. Phys. A **752**, 355 (2005); E. Levin, J. Phys. Conf. Ser. **5**, 127 (2005) [arXiv:hep-ph/0408039].
- [2] J. Jalilian-Marian and Y. V. Kovchegov, Prog. Part. Nucl. Phys. **56**, 104 (2006).
- [3] K. Golec-Biernat and M. Wüsthoff, Phys. Rev. D **59**, 014017 (1999); Phys. Rev. D **60**, 114023 (1999); J. Bartels, K. Golec-Biernat and H. Kowalski, Phys. Rev. D **66**, 014001 (2002).
- [4] A. M. Stasto, K. Golec-Biernat and J. Kwiecinski, Phys. Rev. Lett. **86**, 596 (2001).
- [5] V. N. Gribov and L. N. Lipatov, Yad. Fiz. **15**, 781 (1972) [Sov. J. Nucl. Phys. **15**, 438 (1972)]; Yad. Fiz. **15**, 1218 (1972) [Sov. J. Nucl. Phys. **15**, 675 (1972)]; G. Altarelli and G. Parisi, Nucl. Phys. B **126**, 298 (1977); Yu. L. Dokshitzer, Sov. Phys. JETP **46**, 641 (1977) [Zh. Eksp. Teor. Fiz. **73**, 1216 (1977)]; Yu. L. Dokshitzer, D. Diakonov and S. I. Troian, Phys. Rept. **58**, 269 (1980).
- [6] E. A. Kuraev, L. N. Lipatov and V. S. Fadin, Sov. Phys. JETP **45**, 199 (1977) [Zh. Eksp. Teor. Fiz. **72**, 377 (1977)]; I. I. Balitsky and L. N. Lipatov, Sov. J. Nucl. Phys. **28**, 822 (1978) [Yad. Fiz. **28**, 1597 (1978)].
- [7] E. Iancu, K. Itakura and L. McLerran, Nucl. Phys. A **708**, 327 (2002); A. H. Mueller and D. N. Triantafyllopoulos, Nucl. Phys. B **640**, 331 (2002).
- [8] E. Iancu, K. Itakura and S. Munier, Phys. Lett. B **590**, 199 (2004).
- [9] J. R. Forshaw and G. Shaw, JHEP **0412**, 052 (2004).

- [10] I. Balitsky, Nucl. Phys. B **463**, 99 (1996), Phys. Lett. B **518**, 235 (2001); J. Jalilian-Marian, A. Kovner, A. Leonidov and H. Weigert, Nucl. Phys. B **504**, 415 (1997), Phys. Rev. D **59**, 014014 (1999); E. Iancu, A. Leonidov and L. D. McLerran, Phys. Lett. B **510**, 133 (2001), Nucl. Phys. A **692**, 583 (2001); Y. V. Kovchegov, Phys. Rev. D **60**, 034008 (1999), Phys. Rev. D **61**, 074018 (2000).
- [11] I. Arsene *et al.* [BRAHMS Collaboration], Phys. Rev. Lett. **93**, 242303 (2004).
- [12] G. Rakness [STAR Collaboration], arXiv:hep-ex/0507093.
- [13] J. Adams *et al.* [STAR Collaboration], Phys. Rev. Lett. **91**, 072304 (2003); Phys. Rev. C **70**, 064907 (2004).
- [14] S. S. Adler *et al.* [PHENIX Collaboration], Phys. Rev. Lett. **91**, 072303 (2003).
- [15] D. Kharzeev, Y. V. Kovchegov and K. Tuchin, Phys. Lett. B **599**, 23 (2004).
- [16] A. Dumitru, A. Hayashigaki and J. Jalilian-Marian, arXiv:hep-ph/0506308.
- [17] for the general formalism see, for example, L. V. Gribov, E. M. Levin and M. G. Ryskin, Phys. Rept. **100**, 1 (1983); for applications to Au+Au and d+Au collisions at RHIC see D. Kharzeev and E. Levin, Phys. Lett. B **523**, 79 (2001); D. Kharzeev, E. Levin and M. Nardi, Nucl. Phys. A **730**, 448 (2004) [Erratum-ibid. A **743**, 329 (2004)]; for applications to p+p collisions at RHIC energy see M. Czech and A. Szczurek, Phys. Rev. C **72**, 015202 (2005).
- [18] L. McLerran and R. Venugopalan, Phys. Rev. D **49**, 2233 (1994); *ibid.* **49**, 3352 (1994); Y. V. Kovchegov, *ibid.* **54**, 5463 (1996); *ibid.* **55**, 5445 (1997); A. H. Mueller, Nucl. Phys. A **724**, 223 (2003); J. Jalilian-Marian, A. Kovner, L. D. McLerran and H. Weigert, Phys. Rev. D **55**, 5414 (1997).
- [19] A. Accardi and M. Gyulassy, Phys. Lett. B **586**, 244 (2004).
- [20] R. Baier, Y. Mehtar-Tani and D. Schiff, arXiv:hep-ph/0508026.
- [21] V. Guzey, M. Strikman and W. Vogelsang, Phys. Lett. B **603**, 173 (2004).
- [22] D. Kharzeev, Y. V. Kovchegov and K. Tuchin, Phys. Rev. D **68**, 094013 (2003); J. L. Albacete, N. Armesto, A. Kovner, C. A. Salgado and U. A. Wiedemann, Phys. Rev. Lett. **92**, 082001 (2004); E. Iancu, K. Itakura and D. N. Triantafyllopoulos, Nucl. Phys. A **742**, 182 (2004).
- [23] D. Kharzeev, E. Levin and L. McLerran, Phys. Lett. B **561**, 93 (2003).
- [24] H. L. Lai *et al.* [CTEQ Collaboration], Eur. Phys. J. C **12**, 375 (2000).
- [25] B. A. Kniehl, G. Kramer and B. Pötter, Nucl. Phys. B **582**, 514 (2000).
- [26] F. Gelis and J. Jalilian-Marian, unpublished.
- [27] K. J. Eskola, H. Honkanen, H. Niemi, P. V. Ruuskanen and S. S. Rasanen, Phys. Rev. C **72**, 044904 (2005); K. J. Eskola and H. Honkanen, Nucl. Phys. A **713**, 167 (2003).